SEMICONDUCTOR LASERS

By Robert H. Rediker

Since the announcement of the GaAs diode laser1 in November 1962, laser action has been achieved in diodes of a variety of III-V and IV-VI direct-gap semiconductors.2 The wavelength of the emitted radiation varies over the range from 6300 Å for the III-V mixed semiconductor Ga(As_xP_{1-x}) to 85 000 Å for the IV-VI semiconductor PbSe. The semiconductor diode laser has the advantages that its size is small, that it converts electric power directly into coherent light, and that its output can be modulated by simply modulating the diode current. Figure 1 shows an artist's sketch of a GaAs diode laser in a pill-type package. Such a laser, when operated between 4° and 20°K, has emitted up to 6 W of continuous coherent radiation at close to fifty percent power efficiency,3 and the radiation has been modulated4 at frequencies up to 11 Gc. At room temperature such a laser can be used on a pulse basis and 20 W of coherent radiation can be emitted in 50 nsec pulses.5 When operated continuously at currents not too high above threshold, GaAs lasers can operate stably in one mode of the Fabry-Perot cavity formed by the cleaved face, shown in Fig. 1, and the parallel face on the opposite end of the laser. The width of such a cavity mode has been measured6 to be less than 50 Mc/sec or less than 1.5 parts in 107 of the output frequency.

Because of the advantages mentioned above, injection lasers may find radar, communications, and computer applications, particularly where the absorption of the laser radiation in the atmosphere is unimportant or can be controlled or eliminated. It is possible today, to build a complete roomtemperature GaAs-laser radar-transmitter in the size of a two-cell flashlight which would emit of the order of 10 W of coherent radiation in 10-20 nsec pulses.

Population inversion

In Fig. 2a is shown an equilibrium band diagram of a p-n junction in which both p and n regions have been assumed to be degenerate, as illustrated

Robert H. Rediker is leader of the Applied Physics Group at the Massachusetts Institute of Technology's Lincoln Laboratory, which is operated with Air Force support.

by the Fermi level, ϕ , being below the top of the valence band in the p region and above the bottom of the conduction band in the n region. By applying a forward bias, V, across the junction, a region of population inversion is produced at the junction as illustrated in Fig. 2b. In the inversion region more quanta are emitted than are absorbed in radiative transitions between conduction and valence bands. The number of quanta emitted and absorbed are given by

$$r_{\text{abs}} = A W_{ve} f_v (1 - f_e) \rho(\nu),$$

$$r_{\text{emit}} = A W_{cv} f_e (1 - f_v) \rho(\nu),$$
(1)

 $W_{vc} = W_{cv}$ = the probability per unit time for a transition between a state in the valence band and a state in the conduction band separated by hv.

 $\rho(\nu)$ = density of photons at energy $h\nu$. A = a constant containing the density of states in the valence and conduction bands.

 $f_c(f_v)$ = probability for occupancy of a state in the conduction (valence) band.

Equation 1 must be integrated over all pairs of states separated by $h\nu$. If one makes the common assumptions that the electrons in the conduction band are in thermal equilibrium among themselves and the electrons in the valence band are also in equilibrium with themselves, the population distribution in the two bands can be expressed in terms of quasi-Fermi levels. The quantities f_c and f_v are related to these quasi-Fermi levels ϕ_c and ϕ_v by Fermi-Dirac statistics

$$f = \frac{1}{1 + \exp((E - \phi)/kT)}.$$
 (2)

For stimulated emission to exceed absorption, $r_{\rm emit} > r_{\rm abs}$, substituting (2) into (1), one obtains

$$\phi_c - \phi_v > h\nu. \tag{3}$$

Thus, the condition for population inversion in a junction laser (as first pointed out by Bernard and Duraffourg8) is that the forward voltage applied across the junction, which is equal to $\phi_c - \phi_v$, must be larger than that corresponding to the energy of the emitted radiation.

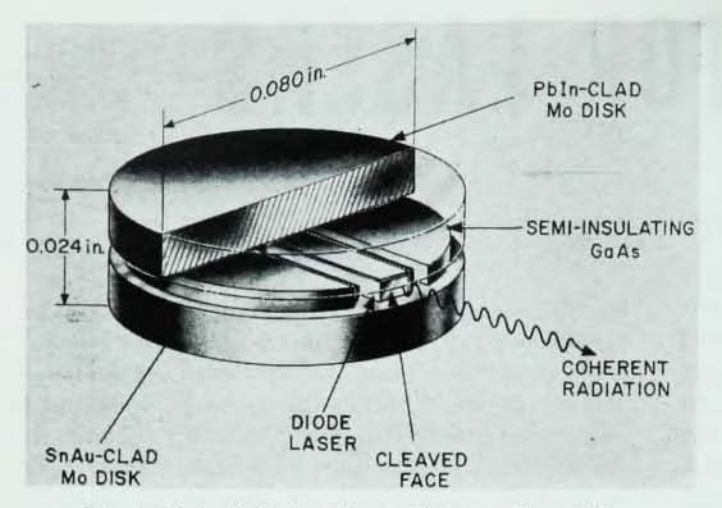


Fig. 1. GaAs diode laser in a pill-type package. Note surface area of the 0.080-inch disk is 1/75 that of an American dime. The diode laser is a rectangular parallelepiped whose dimensions are typically 0.010 inch x 0.030 inch x 0.003 inch thick.

In the above discussion the recombination mechanism has been assumed to be a band-to-band transition. The transitions responsible for laser action will be described in more detail below.

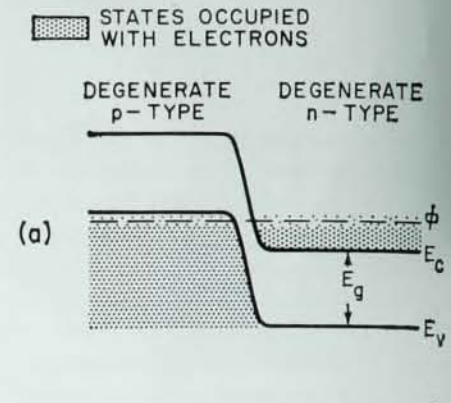
Guided mode laser action

The laser action occurs in even TE or TM modes guided along the plane of population inversion as shown in the idealized model of Fig. 3. Energy is fed into the modes in the inverted population region labeled 1 which is taken to be of width 2w and is assumed to be characterized by a constant negative conductivity of magnitude o1. Energy is lost by the modes in the p and n regions (labeled 2) and 3) on either side of the junction. These regions are characterized by constant positive conductivities σ_2 and σ_3 . By solving the electromagnetic propagation problem, we can determine how far the modes penetrate into the lossy regions 2 and 3 and thus determine how much energy must be supplied in the inverted region before the net flow of energy into the mode is positive and it is amplified as it propagates between the faces of the diode perpendicular to the z direction. These faces, which are shown shaded in the figure, have been cut flat and parallel to each other to form the faces of a Fabry-Perot cavity. The electromagnetic wave has a z, x, and t variation of the usual form.

$$z \text{ variation} = e^{+j\omega t - jkz}$$

$$x \text{ variation} = \begin{cases} A \cos k_1 x + B \sin k_1 x & \text{region 1} \\ e^{+jk_2 x} & \text{region 2} \\ e^{-jk_3 x} & \text{region 3} \end{cases}$$
(4)

If one matches boundary conditions for the continuity of transverse E and H at the two interfaces



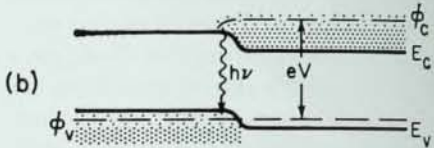


Fig. 2. Energy-band diagram of a p-n junction: (a) Zero applied voltage. (b) Applied voltage $V>E_{\rm g}/e$.

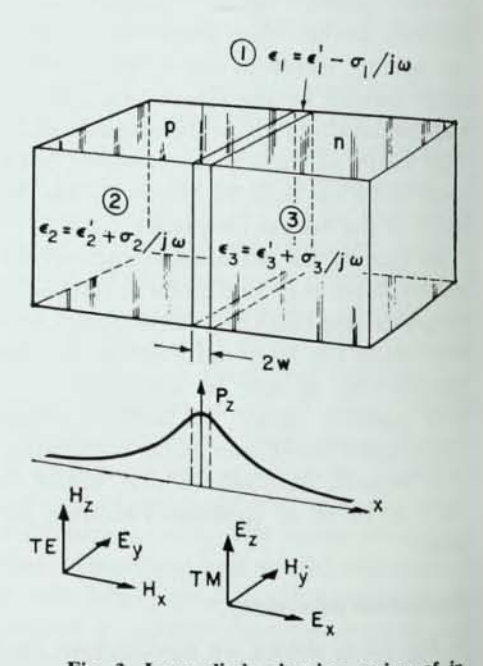


Fig. 3. Laser diode showing region of inverted population at junction labeled (1) and lossy dielectric regions on either side labeled (2) and (3). X-dependence of symmetrical electromagnetic field is also shown. Field components of TE and TM modes are indicated for propagation in z-direction between reflecting faces of Fabry-Perot type cavity.

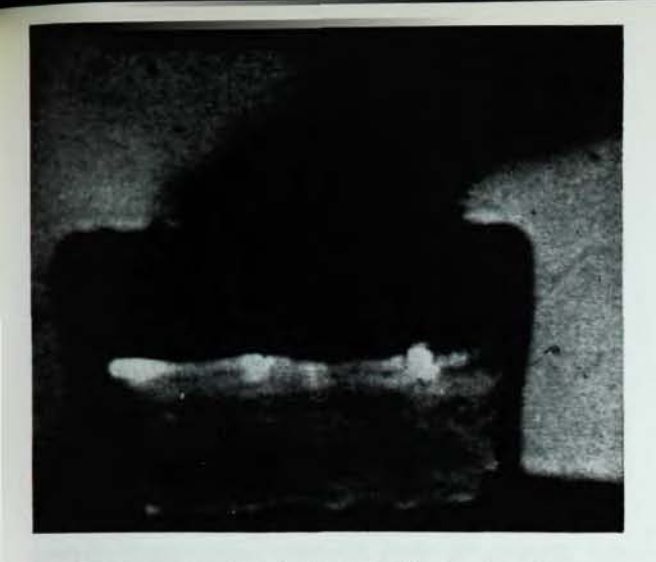


Fig. 4. Photograph of GaAs laser emitting in three filaments (courtesy A. E. Michel)

and makes the pair of assumptions, $\omega^2 \mu_n(\epsilon_1 - \epsilon_2) w^2 << 1$ and σ_2 , $\sigma_3 << \sigma_1 << \omega \epsilon$, both of which are valid for junction lasers, one obtains a simple result for k in terms of σ_1 for both TM and TE waves.

$$k \approx k_0(1 + j\eta/2),$$

$$\eta = \frac{\sigma_2 + \sigma_3}{2\omega\epsilon} - 2(k_0\omega)^2 \frac{\epsilon'_1 - (\epsilon'_2 + \epsilon'_3)/2}{\epsilon} \frac{\sigma_1}{\omega\epsilon}, \quad (5)$$

$$k_0 = \omega \left(\mu_0\epsilon\right)^{\frac{1}{2}}.$$

Thus, with the above approximations, the thresholds for TE and TM waves are calculated to be the same, in agreement with experiment. The real part of the propagation constant k is approximately equal to ko, the propagation constant in the pure semiconductor. The imaginary part of k, which determines the attenuation or growth of the wave, is expressed in terms of η . The first term in the equation for η in (5) gives the rate of decay due to losses in the p and n regions, while the second term gives the rate of growth due to the inverted population in region 1. For the wave to grow, the negative conductivity, o1, must be large enough so that the second term is larger than the first. The penetration of the wave into the lossy regions is determined by

$$\left\lceil \epsilon'_1 - \left(\frac{\epsilon'_2 + \epsilon'_3}{2}\right) \right\rceil$$
.

As can be seen from (5), only if this quantity is positive will the wave be able to grow; as this quantity becomes larger, the penetration into the lossy regions become smaller.

The wave propagates in the z-direction as shown in Fig. 3 between the reflecting faces of the Fabry-Perot cavity. If the rate per unit length at which energy is lost by the wave to the lossy region is characterized by α , and if the rate at which energy is absorbed by the wave in the inverted region is

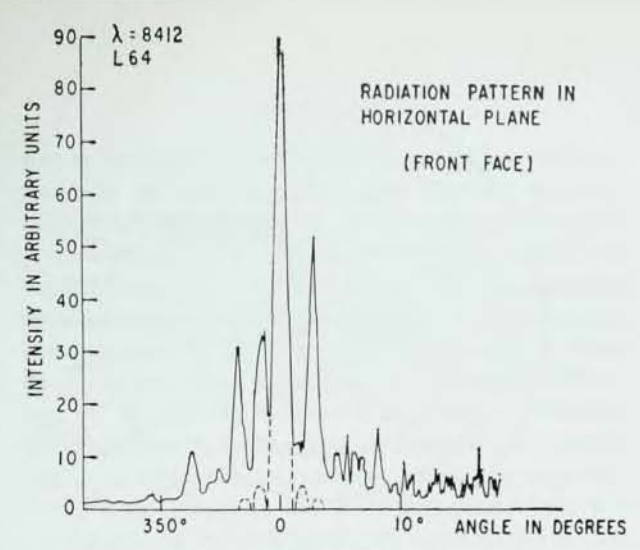


Fig. 5. Radiation pattern in plane of junction of GaAs diode laser at 77°K (reference 14)

characterized by g, the wave will grow if $g > \alpha$. For the diode to act as a laser,

$$R \exp\left[(g - \alpha)L\right] \ge 1,\tag{6}$$

where R is the reflectivity of the faces which form the Fabry-Perot cavity (\sim 32 percent for a GaAs-air interface) and L is the distance between these faces as shown in Fig. 3. The threshold for laser action is from (6):

$$g_t = \alpha + \frac{1}{L} \ln \frac{1}{R}. \tag{7}$$

The quantity g is related to the negative conductivity σ_1 in the inverted region and is in turn determined by the current through the diode which is producing the population inversion. Lasher and Stern¹⁰ have shown that in the limit of low temperatures the threshold current J_t is proportional to g_t :

$$J_t = Cg_t = C(\alpha + \frac{1}{L} \ln \frac{1}{R})$$
. (8)

The threshold current has been measured¹¹ as a function of the length L of the laser cavity and the quantities C and α determined. The value of the quantity a in regions 2 and 3 of Fig. 3 determined from these and other experiments is relatively small, of the order of 10 cm,-1 indicating that the wave does not penetrate far into the lossy n and p regions. The cause of the discontinuity in the real part of the dielectric constant between the active region 1 and the lossy regions 2 and 3, which produces the confinement of the wave, has not been definitely established. Three possible causes have been proposed. First, and probably most important for GaAs, the net impurity density in the region about the p-n junction is less than that of either the p or the n regions unless the junction is extremely abrupt.12 Second, there will be an additional susceptibility in region 1 associated with the negative conductance σ₁ by the Kramer-Kronig

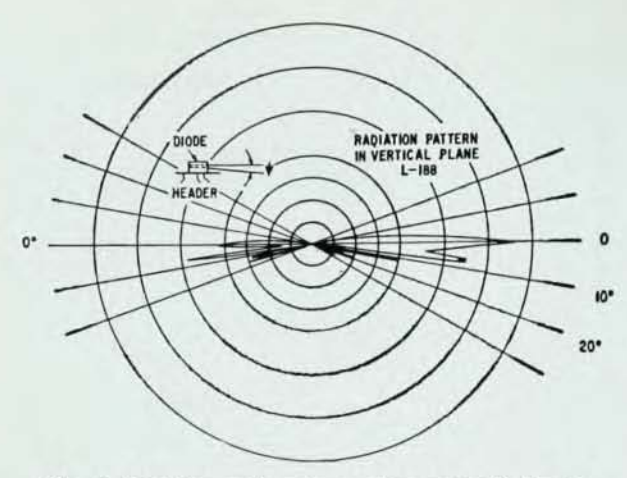


Fig. 6. Radiation pattern in a plane perpendicular to junction of GaAs diode laser at 77°K (reference 14)

relationship.9 Third, there is an absence of free charge in the depletion layer about the junction.¹³ The mode confinement problem still requires further work.

In practice, the guided TE or TM modes propagate in filaments along the junction plane rather than uniformly along the plane as suggested by Fig. 3. Figure 4 is a photograph of a GaAs laser that is radiating from three filaments. This photograph was obtained using an image-converter tube focused on one of the faces defining the Fabry-Perot cavity. The cross-sectional dimensions of the filaments (the area of the spots in Fig. 4) have been determined from radiation patterns. Typical radiation patterns for GaAs lasers are complex and show that the radiation is usually emitted in many beams.14 A radiation pattern in the plane parallel to the junction is shown in Fig. 5 and the corresponding radiation pattern in the plane perpendicular to the junction in Fig. 6. Simpler patterns have been obtained and beam angles as narrow as 1 degree in the plane of the junction and 10 degrees in the perpendicular direction have been reported. Such beam angles correspond (using $d \approx \lambda/\theta$) to a coherently emitting filament of 50µ in the plane of the junction and of 5μ in the plane perpendicular to the junction. The explanation of this filamentary behavior is not completely clear. Similar effects are observed in optically pumped solid-state lasers. Optical inhomogeneities or variations in current density are possible explanations.

Laser threshold conditions

Up to this point we have discussed how to produce an effective inverted population at the plane of a junction and how laser action can occur in guided modes along this plane. An inverted population, however, is not sufficient for laser action. We have already shown that the inversion must be sufficient to overcome losses in the inactive regions (regions 2 and 3 of Fig. 3) and at the reflecting surfaces of the cavity. Losses in the active region must also be overcome. If the probability for transition between appropriate states in the valence and conduction bands $[W_{vc} = W_{cv} \text{ in Eq. (1)}]$ is small, as is true for indirect-gap semiconductors, then other absorption terms must be added to the first equation of (1). Dumke has shown theoretically that, in Ge, absorption due to free carriers would prevent laser action due to band-to-band transitions.

In addition, if nonradiative recombination through localized recombination centers dominates the lifetime of hole-electron pairs, much greater pumping rates are required to establish an effective inverted population than would be necessary if nonradiative processes were not important. Thus, to obtain laser action at realizable diode currents, a semiconductor is desired in which the probability for radiative recombination, $W_{vc} = W_{cv}$, is large. Such diodes will exhibit appreciable luminescence when forward biased. Figure 7 illustrates the spontaneous-emission spectrum obtained from a laser diode when the forward current is below threshold. The width of this spectrum, while narrow as compared to spectra from many luminescent semiconductors, is very much wider than the width of the laser line also shown in Fig. 7. Moreover, the observed laser linewidth is, in this case, determined entirely by the resolution of the spectrometer used. As mentioned in the introduction, laser linewidths of less than 50 Mcps (0.0012 Å) have been measured for GaAs diode lasers.

Theoretically, laser action should occur when the

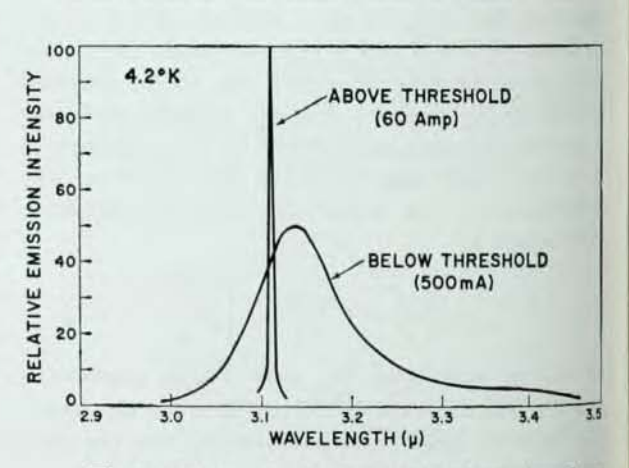


Fig. 7. Spectra of infrared emission from cleaved surface of an InAs diode at 4.2°K. The "broad" spontaneous spectrum obtained below threshold is not drawn to the same intensity scale as the much more intense laser spectrum. The observed width of the laser spectrum was determined by the resolution of the spectrometer used. The difference in wavelength between the peaks of the spontaneous and laser spectra can be explained in part by the shift to lower wavelength of the peak of the spontaneous spectrum as the current is increased.

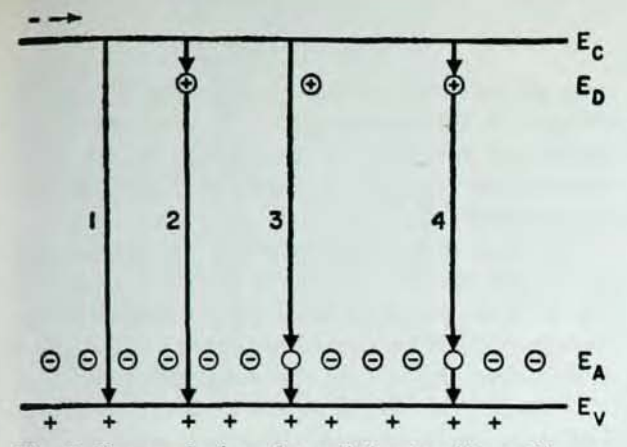


Fig. 8. Four mechanisms for radiative transitions: (1) conduction to valence band; (2) donor to valence band; (3) conduction band to acceptor; (4) donor to acceptor.

intensity of the spontaneous radiation at the lasing wavelength reaches a critical value. This condition, which is equivalent to the gain at the lasing wavelength reaching the critical value, g_t , of (7) and (8), has been experimentally verified for InSb diodes by reducing the linewidth of the spontaneous radiation by application of a magnetic field. Thus, what is required for a semiconductor diode laser is a diode that, when forward biased, efficiently produces radiation in a narrow spectral range.

Up to the time of this writing, laser action has been reported only in direct-gap semiconductors, in which the conduction and valence bands are located at the same point in k-space, and for which $W_{ve} = W_{ev}$ is relatively large. A report¹⁷ of laser action in an indirect-gap semiconductor SiC seems to have been premature. Although, while one may preclude band-to-band laser action in indirect-gap semiconductors, one may not preclude laser action via deep impurity levels if the radiation so produced is sufficiently intense in a narrow spectral region.

The radiative transition

Possible radiative transitions associated with laser action in semiconductors are shown in Fig. 8. In the upper left-hand corner of the figure is shown an electron which has been injected into p-type material. (The injection of an electron into p-type material is for illustrative purposes only.) The p-type material is compensated, as are almost all real semiconductors, there being some donors present as well as the predominant acceptors. The four mechanisms by which the injected electron can recombine with a hole in the valence band and emit the observed infrared radiation are: (1) direct radiative recombination from the conduction band to the valence band; (2) recombination via a donor level—the electron is first captured by one of the compensating donor levels and then makes a radiative transition to the valence band; (3) recombination via an acceptor level—the electron makes a radiative transition to an acceptor level and then recombines with a hole in the valence band; (4) recombination via both a donor and an acceptor level in which the radiative transition is from donor level to acceptor level. In addition, in each of these four mechanisms, there may be the intermediate step of exciton formation. Laser action has been observed over a large range of impurity concentrations. At higher concentrations where the impurity levels form impurity bands which merge into the conduction or valence band and produce band tailing, it may be academic to differentiate between the four mechanisms.

Diode lasers in which the radiation is believed due to band-to-band transitions (mechanism 1) have been reported in lightly doped (N_d ~ 10¹⁶ cm⁻³) GaAs,20 in InAs,21 and in InSb.22 In all these cases the intermediate step of exciton formation could not be excluded. In most lasers of GaAs and InAs. however, the radiation is believed to stem from transitions between the conduction band and an acceptor (zinc) level (mechanism 3). Again, exciton formation cannot be excluded. In the "band-toband" GaAs lasers the energy of the stimulated emission is 1.505 eV (77°K), and this emission is believed to be associated with spontaneous emission whose spectrum can be correlated with the absorption edge by the principle of detailed balance.28 In the "conduction band-to-acceptor" GaAs lasers the energy of the stimulated emission is about 0.020 eV smaller. Similarly, the photon energy associated with the "band-to-band" laser radiation in InAs lasers is 0.020 eV larger than the energy associated with the "band-to-acceptor" laser radiation.21 Thus the mechanism of the radiative transition is not unique; and, even in the same laser diode, it may be possible by changing the junction current to change the recombination mechanism. The mechanisms should be studied for themselves and also with the hope that further understanding may allow us to produce more useful lasers, i.e., lasers in which W_{cv} is larger (the spontaneous line is more intense and narrower) and the threshold current is

Much work is still required to understand the details of the radiative transition, as illustrated by the following example of a problem which may also lead to a better understanding of semiconductor physics. For diodes of heavily doped GaAs (~ 10¹⁸ cm⁻³) the intensity of the high-energy side of the spontaneous recombination line increases with increasing current and the peak intensity shifts to higher energy. This increase has been attributed to

band-filling of the tail produced by the heavy doping in the density of states, but there is disagreement as to whether the tail is in the conduction band or in the valence band. Dumke²⁴ and others interpret the results in terms of a tail in the conduction band, while Bagaev et al.²⁵ insist the tail is in the valence band.

Effects of magnetic field, pressure, temperature

Magnetic field, pressure, and temperature affect the wavelength of the emission from semiconductor injection lasers. The exact wavelength of the laser output is determined by the effective length of the semiconductor cavity,

$$m\lambda = 2nL, \tag{9}$$

where n is the index of refraction of the semiconductor. Thus the wavelength of a given cavity mode, corresponding to a given value of m, will vary as the index of refraction and the length of the cavity. For the near-bandgap laser-radiation, temperature, magnetic field, or pressure changes have a larger fractional effect on n than on the length L.

The cavity mode can be excited only if its wavelength is close to that of the peak of the spontaneous emission (see the section above on laser threshold conditions). For all the transitions shown in Fig. 8 (if the pertinent impurity levels are relatively shallow as they have been in all lasers so far) the spontaneous line will change as the bandgap changes. The temperature, magnetic field, or pressure changes have a larger effect on the bandgap

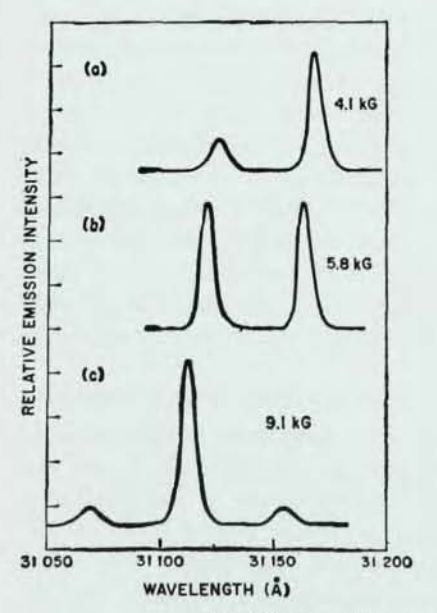


Fig. 9. Spectra of laser emission from cleaved surface of InAs diode at 4.2°K for three different values of magnetic field (reference 26)

than on the cavity modes. Thus there will be small changes in the wavelength of the excited cavity modes and switching of these modes as the spontaneous line "moves through" and excites new cavity modes.

The effect of the magnetic field on the emission wavelength of an InAs diode laser²⁶ is shown in Fig. 9. The wavelength of the individual modes changes by 13 Å because of the change in the index of refraction as the field was increased from 4.1 to 9.1 kG, and the modes switch as described above. The appearance of mode structure, such as illustrated in all three spectra of Fig. 9, is an indication of laser action. The separation between the adjacent modes of a Fabry-Perot cavity (modes which differ by an additional half-wavelength between the reflecting surfaces) is

$$\Delta \lambda = \frac{\lambda^2}{2L[n - \lambda(dn/d\lambda)]},$$
 (10)

and may be correlated with the length of the cavity or may be used to determine more accurately the refractive index and its dispersion.²⁷

In addition to affecting the wavelength of the laser emission, increasing the temperature increases the threshold current for laser action. For most GaAs lasers, the threshold increases slowly with temperature at low temperatures, but above 60°K it increases very nearly as the cube of the temperature. Lasher and Stern10 have shown that this temperature dependence is expected for band-to-band recombination between parabolic bands with no momentum selection rules. Recent results by Dousmanis et al.28 have shown that while the threshold at low temperatures is higher in very heavily doped GaAs, the temperature dependence of the threshold in these materials is lower. They have reported for these heavily doped materials threshold current densities at room temperature of 41 000 A cm-2, which is more than a factor of two smaller than those typically reported for other GaAs diode lasers. The rapid rise of threshold current with temperature has precluded all but short-pulse operation at room temperatures. Studies which might lead towards further understanding of the temperature variation and means of reducing it would increase the practical utility of semiconductor lasers.

New developments

I have described in this paper the semiconductor junction laser. Very recently diode lasers of InSb have been reported²⁹ in which the coherent radiation emanates from the bulk of the semiconductor in which an electron-hole plasma has been established. The possibility of obtaining relatively large

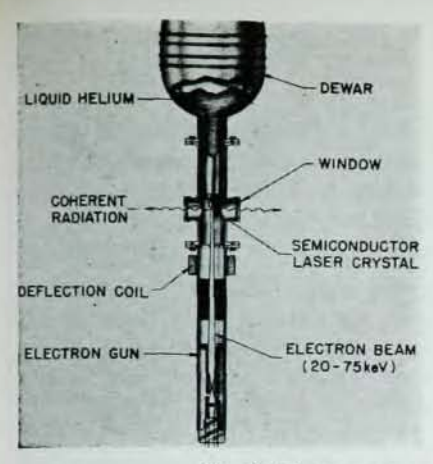


Fig. 10. Electron-gun cryostat system used in electron-beam pumping of semiconductor lasers.

coherently-emitting areas implies smaller beam angles ($\theta \approx \lambda/d$). The large radiating volume is better suited for light amplification, higher output power may be attainable, and, because the population is inverted over a large volume, threshold current densities may be lower.

Also very recently laser action has been reported in InSb,³⁰ InAs,³⁰ GaAs,³¹ and GaSb³² when electron-hole pairs were generated by means of a beam of high-energy electrons as illustrated in Fig. 10. The technique of electron-beam pumping will hopefully permit laser action to be obtained in semiconductors in which it is difficult to produce good *p-n* junctions or in which resistivities are so high that series resistance and consequent heating preclude the use of electrical injection. Typical of these semiconductors are the zinc chalcogenides which, if they lase, will emit in the visible region.

The semiconductor injection laser field is fast moving and it has been difficult for the physics to stay abreast of the technology. However, only if the physics is understood will it be possible to optimize intelligently the semiconductor lasers of the future.

References

- R. N. Hall, G. E. Fenner, J. D. Kingsley, T. F. Soltys, and R. O. Carlson, Phys. Rev. Letters 9, 366 (1962);
 M. I. Nathan, W. P. Dumke, G. Burns, F. H. Dill, Jr., and G. Lasher, Appl. Phys. Letters 1, 62 (1962);
 T. M. Quist, R. H. Rediker, R. J. Keyes, W. E. Krag, B. Lax, A. L. McWhorter, and H. J. Zeiger, Appl. Phys. Letters 1, 91 (1962).
- Ga(As_zP_{1-x}): N. Holonyak, Jr., and S. F. Bevaqua, Appl. Phys. Letters 1, 82 (1962); InAs: I. Melngailis, Appl. Phys. Letters 2, 176 (1963); InP: K. Weiser and R. S. Levitt, Appl. Phys. Letters 2, 178 (1963); (In_xGa_{1-x})As: I. Melngailis, A. J. Strauss, and R. H. Rediker, Proc. IEEE 51, 1154 (1963); InSb: R. J. Phelan, Jr., A. R. Calawa, R. H. Rediker, R. J. Keyes, and B. Lax, Appl. Phys. Letters 3, 143 (1963); C. Benoit à la Guillaume and P. Lavallard, Solid State Commun. 1, 148 (1963); In(As_zP_{1-x}): F. B. Alexander, V. R. Bird, D. R. Carpenter, G. W. Manley, P. S. McDermott, J. R. Peloke, H. F. Quinn, R. J. Riley, and L. R. Yetter, Appl. Phys. Letters 4, 13 (1964); PbTe: J. F. Butler, A. R. Calawa, R. J. Phelan, Jr., T. C. Har-

- man, A. J. Strauss, and R. H. Rediker, Appl. Phys. Letters 5, 75 (1964); PbSe: J. F. Butler, A. R. Celawa, R. J. Phelan, Jr., T. C. Harman, A. J. Strauss, and R. H. Rediker, Solid State Commun. 2, 301 (1964).
- 3. T. M. Quist, private communication.
- B. S. Goldstein and R. M. Weigand, Proc. IEEE, to be published.
- C. C. Gallagher, P. C. Tandy, B. S. Goldstein, J. D. Welch, Proc. IEEE 52, 717 (1964).
- J. A. Armstrong and A. W. Smith, Appl. Phys. Letters 4, 196 (1964).
- G. F. Dalrymple, B. S. Goldstein, and T. M. Quist, Proc. IEEE 52, (1964).
- M. G. A. Bernard and G. Duraffourg, Physica Status Solidi 1, 699 (1961).
- 9. A. L. McWhorter, Solid-State Electronics 6, 417 (1963).
- 10. G. L. Lasher and F. Stern, Phys. Rev. 133, A553 (1964).
- M. Pilkuhn and H. Rupprecht, Proc. IEEE 51, 1243 (1963); M. Pilkuhn, H. Rupprecht, and S. Blum, Solid-State Electron. 5, (1964).
- G. Diemer and B. Bolger, Physica 29, 600 (1963); F. Stern, Symp. Radiative Recombination in Semiconductors, Paris, July 27–28, 1964.
- A. Yariv and R. C. C. Leite, Appl. Phys. Letters 2, 55 (1963).
- G. E. Fenner and J. D. Kingsley, J. Appl. Phys. 34, 3204 (1963).
- 15. W. P. Dumke, Phys. Rev. 127, 1559 (1962).
- R. J. Phelan, Jr., and R. H. Rediker, Symp. Radiative Recombination in Semiconductors, Paris, July 27–28, 1964.
- L. B. Griffiths, A. L. Mlavsky, G. Rupprecht, A. J. Rosenberg, P. H. Smakula, and M. A. Wright, Proc. IEEE 51, 1374 (1963).
- 18. R. N. Hall, Proc. IEEE 52, 91 (1964).
- H. J. Zeiger, J. Appl. Phys. 35, 1657 (1964).
- 20. D. K. Wilson, Appl. Phys. Letters 3, 127 (1963).
- I. Melngailis, Symp. Radiative Recombination in Semiconductors, Paris, July 27–28, 1964.
- R. J. Phelan, Jr., A. R. Calawa, R. H. Rediker, R. J. Keyes, and B. Lax, Appl. Phys. Letters 3, 143 (1963).
- J. C. Sarace, R. H. Kaiser, J. M. Whelan, post-deadline paper, APS Meeting, Washington, D. C., 27–30 April 1964.
- W. P. Dumke, Symp. Radiative Recombination in Semiconductors, Paris, July 27–28, 1964.
- V. S. Bagaev, Y. N. Berozashvili, B. M. Vul, E. I. Zavaritskaya, L. V. Keldysh, and A. P. Shotov, Symp. Radiative Recombination in Semiconductors, Paris, July 27–28, 1964.
- I. Melngailis and R. H. Rediker, Appl. Phys. Letters 2, 202 (1963).
- M. I. Nathan, A. B. Fowler, and G. Burns, Phys. Rev. Letters 11, 152 (1963).
- G. C. Dousmanis, H. Nelson, and D. L. Staebler, to be published.
- I. Melngailis, R. J. Phelan, Jr., and R. H. Rediker, Appl. Phys. Letters 5, 89 (1964).
- C. Benoit à la Guillaume and J. M. DeBever, Symp. Radiative Recombination in Semiconductors, Paris, July 27–28, 1964.
- C. E. Hurwitz and R. J. Keyes, Appl. Phys. Letters 5, 139 (1964).
- C. Benoit à la Guillaume and J. M. DeBever, Compt. Rend., 259, 2200 (1964).